33rd Annual International Conference of the IEEE EMBS
Boston, Massachusetts USA, August 30 - September 3, 2011

Hexagonal Adaptive Filtering on Compound Ultrasound Images

Sonia H. Contreras Ortiz, Tsuicheng Chiu, and Martin D. Fox.

Abstract*—This paper describes an approach to improve the contrast and signal to noise ratio on ultrasound images. Images with sub-pixel lateral displacements were re-sampled using a hexagonal grid, registered and compounded. The resultant image was filtered using a hexagonal adaptive masking filter. This approach was evaluated with simulated images and real images from a breast phantom. The results show total improvements in signal to noise ratio of up to 313% in simulated images, and 182% in phantom images. Contrast to noise ratio was improved by 286% in simulated images and 56% in phantom images.

I. Introduction

Ultrasound images are affected by many types of artifacts that reduce their quality and limit their usefulness. Examples of these artifacts include: speckle, thickness of the image plane, reverberation, shadowing, attenuation and speed of sound errors [1]. Since ultrasound is a safe and cost-effective imaging modality, many efforts have been done to improve the quality of the images. There are two main approaches that have been used to improve signal to noise ratio (SNR) on ultrasound images: compounding and filtering [2].

Compounding is a methodology that combines images acquired from different angles or aperture positions, or using two or more frequencies, with the purpose of averaging out speckle. By combining N images, the reduction in speckle can be up to $\sqrt{N}$ when the images are independent [3].

In spatial compounding the images are typically acquired by rotating the transducer or the sample and registered (aligned) before combined [4, 5]. The images can also be acquired by displacing the transducer laterally [6] or using a combination of lateral and angular displacements [7].

With respect to filtering, conventional linear filtering techniques are often not effective for ultrasound images. There are two main reasons to that: first, the point spread function (PSF) of ultrasound is not shift invariant. And second, noise in ultrasound images can be modeled as having two components: one additive (such as electronic and thermal noise) and other multiplicative (speckle), and the statistics of speckle in the image depend on the physical properties of the tissues.

Previous works have used filtering techniques that include adaptive filters based on local statistics [8-11], anisotropic diffusion [12-14] and wavelets [15, 16].

Statistical adaptive filters are basically smoothing filters designed so that regions within the image that closely resemble the statistics of speckle are replaced by a local mean value, while regions with properties that are least similar to speckle are kept unaltered. The filter output is usually determined by:

$$y = \bar{x} + c\left(x - \bar{x}\right) \tag{1}$$

Where $\bar{x}$ is the mean value of the intensity within the filter window and c is the adaptive filter coefficient, which is calculated based on local statistics. If $c > 1$, the image is sharpened, if $c = 1$, the filter becomes an identity filter, if $0 < c < 1$, the image is smoothed. And in the extreme case, when $c = 0$, the filter output is equal to the local mean.

One of the limitations of masking filters is the window shape. They typically use rectangular windows that cause distortion in curved edges. This paper presents an approach to reduce noise and enhance contrast in ultrasound B-scans that consists of the combination of spatial compounding and hexagonal adaptive filtering. Spatial compounding can reduce speckle and other artifacts and has the potential of improving the PSF. By pre-processing the images using compounding, the effectiveness of signal processing techniques such as filtering can be improved.

II. Background

A. Statistics of Speckle

Ultrasound speckle results from the accumulation of random scatterings in the tissue volume that is being imaged. This accumulation can be described geometrically as a random walk of component phasors [17]. The scattering from these targets undergoes constructive and destructive interference that results in intensity fluctuations in the image that degrades its quality.

Fully developed speckle occurs when the number of scatterings per resolution cell is large (N > 10). In this case, speckle can be modeled using the Rayleigh distribution and its SNR is 1.92 [3]. Speckle has also been modeled using the K- and Rician distributions for partially and fully structured regions respectively [10, 17]. However, when ultrasound signals are logarithmically compressed, their statistics change, and fully developed speckle can be better described using the extreme value distribution, also known as Fisher-Tippett distribution [18] or the Gaussian distribution [13].

Manuscript received March 31st 2011.

S. H. Contreras Ortiz is with the Biomedical Engineering Program at University of Connecticut, 260 Glenbrook Road, Unit 2247 Storrs, CT 06269 USA, on leave from Universidad Tecnologica de Bolivar, Cartagena, Colombia (e-mail: soniac@ engr.uconn.edu).

T. Chiu is with the Biomedical Engineering Program at University of Connecticut, 260 Glenbrook Road, Unit 2247. Storrs, CT 06269 USA (e-mail: tsui-cheng.chiu@uconn.edu).

M. D. Fox is with the Department of Electrical and Computer Engineering, University of Connecticut, 371 Fairfield Way; Unit 2157 Storrs, Connecticut 06269 USA (e-mail: fox@engr.uconn.edu).

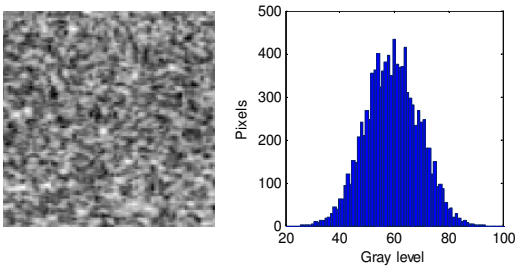

Fig. 1. Left: region of speckle in the image of a contrast phantom. Right: histogram.

The logarithmically compressed envelope signal can be written as

$$X = D\ln(A) + G \tag{2}$$

D is related to the dynamic range of the input and G to the gain of the compressor. Fig. 1 shows a region of speckle from the image of a contrast phantom and its histogram.

The first works on statistical adaptive filters to remove speckle were published in the 1980s. The majority of these filters use the local variance to quantify the extent of speckle formation. Some of the most important contributions are mentioned next. Lee [8] developed masking filters for additive and multiplicative noise based on the local mean and variance, and used them to reduce speckle while preserving edges in radar images. Later on, Bamber and Daft [9] proposed an unsharp masking filter that used the ratio of the local variance to the local mean as the speckle recognition feature. Dutt and Greenleaf [10] focused their research in logarithmically compressed images. They studied the statistics of fully developed speckle and partially developed speckle and proposed an adaptive unsharp masking filter. Finally, Tay *et al.* [11] recently proposed an iterative despeckling method that smoothes only outlying pixel values. Outliers are defined as local extrema and are replaced by the local mean calculated without using the outlier values.

B. Hexagonal Image Processing

Regular hexagonal lattices are optimal for sampling circularly band-limited two-dimensional signals because the spectrum is more efficiently arranged in the frequency domain [19]. As most of medical images are isotropically band-limited, hexagonal sampling is the most appropriate sampling strategy for these images [20].

Most image acquisition and display systems are designed for rectangular pixels. A simple way to create a hexagonal sampling grid is by using rectangular pixels that are displaced by half a pixel on alternate rows (brick wall approach). We named this technique interlaced sampling and explored its implementation in a previous research report [21]. Interlaced sampling can be more robust than rectangular sampling with respect to under-sampling artifacts at high frequencies.

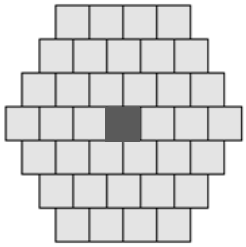

Fig. 2. 7x7 hexagonal mask. The filter's output was assigned to the center pixel (shown in dark gray).

III. Materials and Methods

A. Processing of Simulated Images

The images for this experiment were generated using the ultrasound simulation software Field II [22, 23]. The program used a 3.5 MHz linear transducer composed of 192 elements to generate images of a phantom with some water-filled cysts and high-scattering regions. One of these images is shown in Fig. 4.

1) Spatial compounding: Ten images were generated by displacing the lateral position of the scatterers in 0.05mm steps [21]. The images were registered and re-sampled on an interlaced grid. This operation requires down-sampling by a factor of 2. The interlaced images were defined and displayed using hyper-pixels composed of four pixels (2x2). Alternate sampling lines were shifted one pixel to obtain the interlaced grid. The compound image was obtained by averaging the interlaced images.

2) Adaptive filtering: A statistical adaptive filter similar to the filter proposed by Dutt and Greenleaf [10] was used to process the compound image. A hexagonal mask of size 7x7 pixels was defined as shown in Fig. 2.

The filter's output was calculated using equation (1), and the adaptive filter coefficient c was estimated as follows

$$c = 1 - k/\sigma_x^2 \tag{3}$$

Where σ_x^2 is the local variance, and k is its normalization constant. The value of k was calculated as $k = \sigma_s^2$, where σ_s^2 is the variance in a homogeneous region of the image containing speckle.

The filter's response adapts to the local statistics of the image. A high variance value suggests that there is a boundary in the region and the output of the filter is approximately equal to the input. On the other hand, low variance is a sign that the region is homogeneous, so it is smoothed to reduce noise. The values of c were restricted to be in the interval [0, 1].

B. Processing of Phantom Images

The images for this experiment were from a breast biopsy phantom (Model BB-1, ATS laboratories, Bridgeport, CT). The phantom was in a water tank as shown in Fig. 3. It was imaged with the General Electric RT 3200 scanner (GE Healthcare, Milwaukee, WI) using a 7.5-MHz linear transducer. The images were digitized with 8-bit resolution

Fig. 3. Experimental setup. The breast phantom is in a water bath and the ultrasound transducer is held by a mechanical device.

using a NI IMAQ PCI 1408 board (National Instruments, Austin, TX).

1) Spatial compounding: The transducer was held by a mechanical device that allowed precise lateral shifts (shown in Fig. 3). It was displaced laterally in 0.1mm steps to acquire 20 images from the same section. The images were registered by adding a pseudo-phase and calculating the cross-correlation function, as described in a previous research report [24]. The registering process involves up-scaling of the images by a factor of 4 in order to have sub-pixel precision in the registration. The registered images were re-sampled on an interlaced grid and displayed using 2x2 hyper-pixels. The compound image was calculated by averaging the 20 interlaced images.

2) Adaptive filtering: The compound image was filtered using the same hexagonal masking filter applied to the simulated image. The output of the filter was calculated based on equations (1) and (3). The local variance was used to estimate the speckle content and adjust the smoothing ability of the filter.

IV. Results

A. Using Simulated Images

Fig. 4 shows one of the simulated images and Fig. 5 shows the compound and filtered images. Speckle noise was significantly reduced by compounding, and the adaptive filter further improved the quality of the image. The structures in the filtered image are better delineated.

The SNR and contrast to noise ratio (CNR) were estimated for the original, the compound and the filtered images, and the results are in Table I. The SNR was calculated as the ratio of the mean to the standard deviation within homogeneous regions and the CNR was calculated using the following expression

$$CNR = \frac{|\bar{x} - \bar{y}|}{\sqrt{0.5\left(\sigma_x^2 + \sigma_y^2\right)}} \qquad (4)$$

Where $\bar{x}$ and $\bar{y}$ are the average amplitudes of the object and its background respectively, and σ_x^2 and σ_y^2 are their variances.

Table I shows that after compounding, the improvements

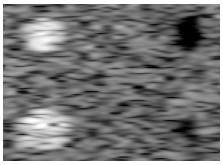

Fig. 4. Simulated image of a cyst phantom showing two hyper-echoic regions and two cysts.

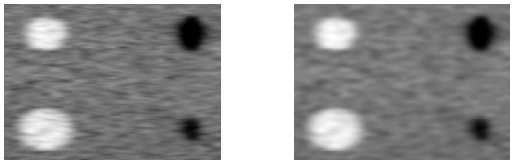

Fig. 5. Interlaced images obtained after processing simulated images of a cyst phantom. Left: compound image. Right: filtered image.

TABLE I
SNR and CNR in Simulated Images

Image	SNR (background)	SNR (hyper-echoic mass)	CNR
Original image	3.89 ± 0.46	8.62 ± 1.84	3.52 ± 0.30
Compound image	11.76 ± 1.04	25.31 ± 3.19	10.69 ± 0.65
Filtered image	16.10 ± 1.74	32.48 ± 3.56	13.65 ± 0.90

in SNR are close to the maximum expected by combining 10 independent images ($\sqrt{10} \approx 3.16$) [3]. The reason is that simulation ensures statistical independence of the averaged images. Improvement in CNR was 200%. The adaptive filter further improved SNR in the background and in the hyper-echoic mass about 36% and 28% respectively; and CNR further increased 27%.

B. Using Phantom Images

Fig. 6 shows one of the images of the breast phantom and Fig. 7 shows the compound and filtered images. Speckle noise was reduced by compounding, especially in the cyst region. The adaptive filter was able to further improve SNR in the image without blurring edges, and enhanced micro-calcifications.

The estimated values for SNR and CNR are shown in Table II. Compounding improved SNR in the background and in the cyst about 18% and 130% respectively. And CNR increased 20%. After hexagonal filtering, the SNR was further improved 31% in the background, 21% in the cyst and CNR increased 30%.

C. Using a Rectangular Filter

The images acquired with the ultrasound scanner were compounded and filtered in their original rectangular sampling grid. The purpose was to compare the performance of the hexagonal filter with a rectangular filter that has the same input-output relation and equivalent size (7x7 pixels). Results show similar improvements in SNR and CNR by compounding. However, the hexagonal filter was more effective in reducing speckle noise when compared to the rectangular filter. After rectangular filtering, the SNR was

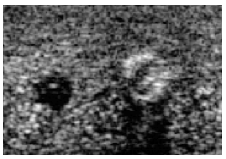

Fig. 6. One of the images of the breast phantom showing a water-filled cyst and a complex mass.

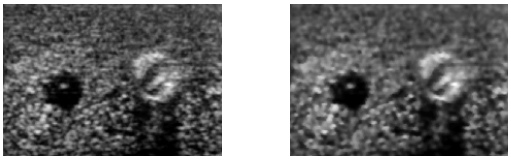

Fig. 7. Interlaced images of the breast phantom. Left: compound image. Right: filtered image.

TABLE II
SNR AND CNR IN PHANTOM IMAGES

Image	SNR (background)	SNR (hypo-echoic mass)	CNR
Original image	4.62 ± 0.33	4.00 ± 0.77	3.76 ± 0.30
Compound image	5.48 ± 0.40	9.28 ± 4.90	4.55 ± 0.20
Filtered image	7.24 ± 0.63	11.30 ± 3.99	5.92 ± 0.33

improved 11% in the background, 14% in the cyst and CNR increased 11%.

V. DISCUSSION AND CONCLUSIONS

The results of this research show that the combination of spatial compounding and adaptive filtering can be very effective to reduce artifacts in ultrasound images. The improvement in overall image quality due to compounding was higher in simulated images than in real images. The reason is that simulated images are statistically independent. The phantom images, on the other hand, were acquired with small lateral displacements, so they are partially correlated. Future work includes the use of angular compounding on images with low correlation to improve the effectiveness of this technique in reducing speckle and other artifacts.

Even though most of the acquisition and display systems for ultrasound images use rectangular grids, there are other sampling methods that are more efficient. This paper proposes a hexagonal masking filter to reduce speckle in compound images. The filter size was chosen as 7x7 pixels to have good noise removal without blurring the structures. Compared to the equivalent rectangular filter, the hexagonal filter is more effective to reduce noise but the processing time is longer.

The combination of compounding and hexagonal processing has the potential of improving the detectability of structures imaged with conventional ultrasound scanners. Applications of this approach include the pre-processing of medical images for automatic segmentation and analysis.

REFERENCES

[1] F. W. Kremkau and K. J. W. Taylor, "Artifacts in ultrasound imaging," *Journal of Ultrasound in Medicine,* vol. 5, pp. 227-237, 1986.

[2] J. C. Gatenby, J. C. Hoddinott, and S. Leeman, "Phasing out speckle," *Physics in Medicine and Biology,* vol. 34, pp. 1683-1689, 1989.

[3] C. B. Burckhardt, "Speckle in Ultrasound B-Mode Scans," *Sonics and Ultrasonics, IEEE Transactions on,* vol. 25, pp. 1-6, 1978.

[4] G. R. Bashford and J. L. Morse, "Circular ultrasound compounding by designed matrix weighting," *IEEE Transactions on Medical Imaging,* vol. 25, pp. 732-741, 2006.

[5] C. Hansen, N. Hüttebräuker, W. Wilkening, S. Brunke, and H. Ermert, "Full angle spatial compounding for improved replenishment analyses in contrast perfusion imaging: In vitro studies," *IEEE Transactions on Ultrasonics, Ferroelectrics, and Frequency Control,* vol. 55, pp. 819-830, 2008.

[6] G. E. Trahey, S. W. Smith, and O. T. von Ramm, "Speckle Pattern Correlation With Lateral Aperture Translation: Experimental Results And Implications For Spatial Compounding," *Modelling, Measurement and Control A,* vol. UFFC-33, pp. 257-264, 1986.

[7] M. Vogt and H. Ermert, "Limited-angle spatial compound imaging of skin with high-frequency ultrasound (20 MHz)," *IEEE Transactions on Ultrasonics, Ferroelectrics, and Frequency Control,* vol. 55, pp. 1975-1983, 2008.

[8] J.-S. Lee, "Digital Image Enhancement and Noise Filtering by Use of Local Statistics," *Pattern Analysis and Machine Intelligence, IEEE Transactions on,* vol. PAMI-2, pp. 165-168, 1980.

[9] J. C. Bamber and C. Daft, "Adaptive filtering for reduction of speckle in ultrasonic pulse-echo images," *Ultrasonics,* vol. 24, pp. 41-44, 1986.

[10] V. Dutt and J. F. Greenleaf, "Adaptive speckle reduction filter for log-compressed B-scan images," *Medical Imaging, IEEE Transactions on,* vol. 15, pp. 802-813, 1996.

[11] P. C. Tay, C. D. Garson, S. T. Acton, and J. A. Hossack, "Ultrasound Despeckling for Contrast Enhancement," *Image Processing, IEEE Transactions on,* vol. 19, pp. 1847-1860, 2010.

[12] Y. Yongjian and S. T. Acton, "Speckle reducing anisotropic diffusion," *Image Processing, IEEE Transactions on,* vol. 11, pp. 1260-1270, 2002.

[13] K. Z. Abd-Elmoniem, A. B. M. Youssef, and Y. M. Kadah, "Real-time speckle reduction and coherence enhancement in ultrasound imaging via nonlinear anisotropic diffusion," *IEEE Transactions on Biomedical Engineering,* vol. 49, pp. 997-1014, 2002.

[14] K. Krissian, C. F. Westin, R. Kikinis, and K. G. Vosburgh, "Oriented Speckle Reducing Anisotropic Diffusion," *Image Processing, IEEE Transactions on,* vol. 16, pp. 1412-1424, 2007.

[15] S. Gupta, R. Chauhan, and S. Sexana, "Wavelet-based statistical approach for speckle reduction in medical ultrasound images," *Medical and Biological Engineering and Computing,* vol. 42, pp. 189-192, 2004.

[16] Z. Xuli, A. F. Laine, and E. A. Geiser, "Speckle reduction and contrast enhancement of echocardiograms via multiscale nonlinear processing," *Medical Imaging, IEEE Transactions on,* vol. 17, pp. 532-540, 1998.

[17] R. F. Wagner, S. W. Smith, J. M. Sandrik, and H. Lopez, "Statistics of Speckle in Ultrasound B-Scans," *Sonics and Ultrasonics, IEEE Transactions on,* vol. 30, pp. 156-163, 1983.

[18] D. Kaplan and Q. Ma, "On the statistical characteristics of log-compressed Rayleigh signals: Theoretical formulation and experimental results," *Journal of the Acoustical Society of America,* vol. 95, pp. 1396-1400, 1994.

[19] R. M. Mersereau, "The processing of hexagonally sampled two-dimensional signals," *Proceedings of the IEEE,* vol. 67, pp. 930-949, 1979.

[20] J. C. Ehrhardt, "MR data acquisition and reconstruction using efficient sampling schemes," *IEEE Transactions on Medical Imaging,* vol. 9, pp. 305-309, 1990.

[21] S. H. Contreras Ortiz, J. J. MacIone, and M. D. Fox, "Enhancement of ultrasound images by displacement, averaging, and interlacing," *Journal of Electronic Imaging,* vol. 19, 2010.

[22] J. A. Jensen and N. B. Svendsen, "Calculation of pressure fields from arbitrarily shaped, apodized, and excited ultrasound transducers," *IEEE Transactions on Ultrasonics, Ferroelectrics, and Frequency Control,* vol. 39, pp. 262-267, 1992.

[23] J. A. Jensen, "FIELD: A program for simulating ultrasound systems," *Medical and Biological Engineering and Computing,* vol. 34, pp. 351-352, 1996.

[24] S. H. Contreras, J. Macione, and M. D. Fox, "Displacement estimation in ultrasound images using pseudo-phase," in *Bioengineering Conference, 2009 IEEE 35th Annual Northeast*, 2009, pp. 1-3.